

Industrial Wind Erosion: PM Emission from the Erodible Flat Surfaces of Tailing Basins



V. Dentoni, B. Grosso, G. Massacci, M. Cigagna, C. Levanti,
C. Corda and F. Pinna

1 Introduction

The emission of particulate matter (PM) from industrial sites typically derives from both conveyed sources (chimneys, dust collectors, etc.) and fugitive dust sources (material handling and transportation, heap formation, transit of vehicles along unpaved roads, wind erosion, etc.). While the emission from conveyed sources is relatively easy to estimate, the characterization of fugitive sources requires the knowledge of the physical properties of the handled/deposited material, the transportation cycle, and the type of machinery in use, as well as the anemological conditions of the site under consideration.

The dust flow deriving from fugitive sources is generally calculated as the product of the *action intensity* for a specific parameter (*Emission Factor*), which takes into account the source physical characteristics. The dust flow (kg/h) generated by handling operations of granular material is calculated, for example, as a product of the mass of material moved in the time unit (*action intensity*) by an *Emission Factor* (EF) that indicates the kilograms of dust emitted for each kilogram of material moved. The dust flow (kg/h) generated by earth moving vehicles travelling along unpaved roads (kg/h) is calculated as the product of the road length travelled in the time unit (*action intensity*) by an emission factor (EF) that indicates the kilograms of dust emitted by a road length unit (kg/km).

Dust emission caused by wind erosion is not linked to specific industrial operations but only to the wind action over the exposed surfaces of the material

V. Dentoni (✉) · B. Grosso · G. Massacci · C. Corda · F. Pinna
DICAAR—Department of Civil and Environmental Engineering
and Architecture, University of Cagliari, Via Marengo 2, Cagliari, Italy
e-mail: vdentoni@unica.it

M. Cigagna · C. Levanti
CINIGEO—Consorzio Interuniversitario Nazionale per l'Ingegneria
delle Georisorse, Rome, Italy

© Springer Nature Switzerland AG 2019

E. Widzyk-Capehart et al. (eds.), *Proceedings of the 18th Symposium on Environmental Issues and Waste Management in Energy and Mineral Production*, https://doi.org/10.1007/978-3-319-99903-6_2

accumulated outdoor (heaps, dumps, tailing basins, etc.). The effect of the wind action depends on factors such as the extent and orientation of the deposit surfaces, the grain size and moisture content of the deposited material, and the anemological conditions of the specific site under exam. From this point of view, dust emission from tailing basins could be quite significant, due to both the extent of the basin surfaces exposed to wind and the small particle size of the disposed material.

The present article specifically deals with the emission of PM from the deposits of mineralogical processing residue. In fact, the examination of the technical and scientific reports has shown that the emission factors proposed for other types of erodible surfaces cannot be directly applied to those deposits, because of their peculiar characteristics: wide and flat surfaces with low roughness and residue physical state dependent on its moisture content.

The object of the research hereby discussed is the definition of an emission conceptual model applicable to the bauxite residue disposal areas (BRDA). In particular, based on the analysis of the scientific literature regarding wind erosion, the article proposes a specific-site conceptual model and its validation procedure.

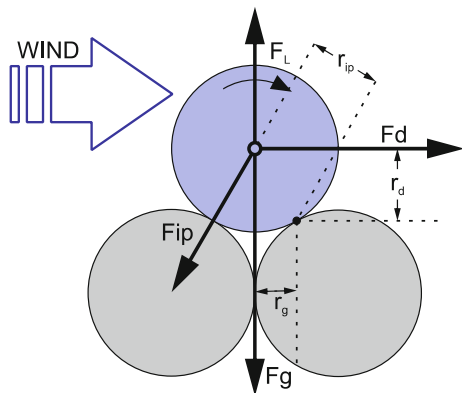
2 Wind Erosion

The evaluation of the dust flow generated by wind erosion is particularly complex and is typically based on the development of specific-site conceptual models. The parameters that influence the erosion phenomenon are, in fact, numerous and of complex evaluation, so that general emission models only interpret the main laws governing the phenomenon, while the most complex and detailed aspects are taken into account by using constant parameters, whose values are decisive for each specific case study.

The comprehension of the wind erosion mechanism is of primary importance in the studies of landscape dynamics (formation or erosion of dunes, beaches, etc.), when analyzing problems of soil impoverishment in agricultural areas or assessing the environmental impact arising from industrial activities. In all cases mentioned above, the erosion phenomenon causes the emission and dispersion of granular materials composed of free inorganic particles. In the field of geological sciences, particles between 60 and 2000 μm moving in contact with the ground are of primary interest. Environmental and health impact studies consider smaller particles (PM_{10} and $\text{PM}_{2.5}$), as they are transported in suspension by the air and, most important, they might be capable of penetrating the inner parts of the human respiratory system.

The lifting mechanism of a solid particle is governed by the wind speed and by the particle size and density. The lifting action is explained by the drag force (F_d) and lifting force (F_L) exerted by the wind, which are opposed by the gravitational force (F_g) and by the surface adhesion force (F_{ip}). Shao and Lu (2000) described the motion trigger mechanism with reference to the scheme in Fig. 1.

Fig. 1 Motion trigger mechanism described by Shao and Lu (2000)



A particle, initially in contact with others, is displaced by the wind when the moment of the forces exerted on its surface (F_d and F_L) with respect to the support point P equals the moment of the resisting forces (F_g and F_{ip}); that condition is expressed by Eq. (1):

$$r_d F_d \approx r_g (F_g - F_L) + r_{ip} F_{ip}. \quad (1)$$

Equation (2) is the expression of the threshold friction velocity (u_{*ft}) obtained from Eq. (1) by replacing the forces' mathematical formulas (Bagnold 1941):

$$u_{*ft} = A_{ft} \sqrt{\frac{\rho_p - \rho_a}{\rho_a} g D_p}. \quad (2)$$

where ρ_p and ρ_a are, respectively, the particle and the fluid density, D_p is the particle diameter, g is gravity acceleration, and A_{ft} is a function of the interparticle forces, the suspension forces, and the Reynolds number.

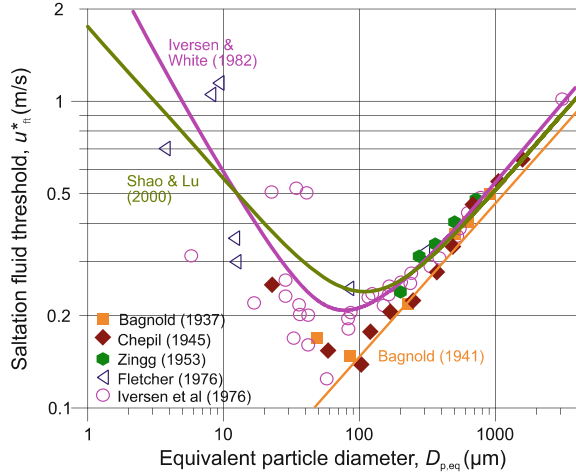
Wind erosion only occurs when the friction velocity exceeds the threshold friction velocity (u_{*ft}). By applying Eq. (2) to a series of experimental data for dissolved sand, Bagnold obtained $A_{ft} = 0.10$ (Bagnold 1941). Using the A_{ft} function proposed by Iversen and White (1982), Shao and Lu (2000) suggested the use of Eq. (3):

$$u_{*ft} = A_N \sqrt{\frac{\rho_p - \rho_a}{\rho_a} g D_p + \frac{\gamma}{\rho_a D_p}}. \quad (3)$$

where γ accounts for the interparticle forces and A_N for the suspension forces and the Reynolds number.

Figure 2 shows the variability of the *threshold friction velocity* as a function of the particle equivalent diameter (Kok et al. 2012). The diagram integrates the research results of various authors: Bagnold (1937), Chepil (1945), Zingg (1953), and Iversen et al. (1976) for sand and dust particles; Fletcher (1976) and Iversen

Fig. 2 Saltation fluid velocity as a function of the saltators' size (Kok et al. 2012)



et al. (1976) for other materials. The models proposed by Iversen and White (1982), Shao and Lu (2000), and Bagnold (1941) are also integrated in Fig. 2, while the effect of the particle density is included in the definition of the particle equivalent diameter given by Eq. (4):

$$D_{p,eq} = \frac{D_p \rho_p}{\rho_{p,sand}}. \quad (4)$$

where ρ_p is the density of the particle and $\rho_{p,sand}$ is equal to 2650 kgm^{-3} .

Figure 2 shows that larger ($D_p > 500 \mu\text{m}$) and smaller particles ($D_p < 10 \mu\text{m}$) are hardly raised by the wind (i.e., they are raised when the wind takes very high speed), due to their weight in the first case and to the adhesion forces in the second case (Kok et al. 2012). The minimum value of the *threshold friction velocity* (*saltation fluid threshold*) is for particle diameters around $100 \mu\text{m}$.

According to Bagnold (1941) and Shao (2008), as the wind speed increases particles with equivalent diameter around $100 \mu\text{m}$ are lifted in the air; after a short trajectory, they fall onto the surface bouncing several times (*saltation*); the impact with the surface breaks the interparticle bonds releasing smaller particles, which remain suspended in the air, because of their lightness, to be transported by the wind even at considerable distances (*suspension*). The impact of bouncing particles also determines the transfer of momentum to larger particles (between 100 and $500 \mu\text{m}$), which are not transported in suspension but move in contact with the surface (*creeping or reptation*).

In line with the above-described conceptual model, wind erosion develops according to the following mechanisms: transport in suspension for long distances ($D_d < 20 \mu\text{m}$), transport in suspension for short distances ($20 \mu\text{m} < D_d < 70 \mu\text{m}$), saltation ($70 \mu\text{m} < D_d < 100 \mu\text{m}$), and creeping or reptation ($D_d > 500 \mu\text{m}$).

Clearly, the attribution of the type of motion to the particle size class depends on the wind speed and is therefore purely indicative.

3 PM Emission

Tailings of metallurgical processes and specifically those deriving from the bauxite treatment (red mud) are composed of very small particles (Type A): 90% of the red mud is typically below 20 μm . Due to the superficial forces, small loose particles (Type A) tend to aggregate to form macro-particles (Type B) with diameter between 20 and 300 μm (Alfaro et al. 1997).

Dust emission from tailing deposits is generated by the following mechanisms:

- direct lifting of loose particles (Type A);
- expulsion of loose particles from the surface due to the impact of macro-particles (Type B), which play the role of saltators (bouncing particles);
- disintegration of bouncing macro-particles (Type B) into loose particles (Type A), as a result of their impact on the surface.

Since the threshold velocity of the macro-particles (Type B) is lower than that of the smaller loose particles (Type A), the emission is triggered by the saltation of macro-particles with equivalent diameter around 100 μm and subsequently, when the wind speed increases, by the lifting of smaller loose particles (Type A) and bigger macro-particles (Type B), according to Fig. 2. The mathematical expressions describing the *saltation threshold velocity* and the dust emission flow refer to the mechanisms described above.

3.1 Threshold Shear Velocity

The general expression of the *saltation threshold velocity* is given by Shao and Lu (2000), with an adjustment that takes into account the effect of the particles' physical characteristics and, in particular, their moisture content (as it determines the onset of interparticle forces that inhibit saltation). Fécan et al. (1999) suggested the use of Eq. (5):

$$\frac{u_{*wt}}{u_{*ft}} = 1 (w < w'),$$

$$\frac{u_{*wt}}{u_{*ft}} = \sqrt{1 + 1.2(w - w')^{0.68}} (w \geq w').$$
(5)

where u_{*wt} is the *threshold friction velocity* for a given moisture content (w); w' is the humidity at which the development of the capillary forces occurs and depends on the clay fraction in the soil (c_s), according to Eq. (6) (Fecan et al. 1999):

$$w' = 0.17c_s + 0.0014c_s^2. \quad (6)$$

3.2 Emitted Dust Flow

The dust flow ($\text{kg/m}^2\text{s}$) is proportional to the kinetic energy transferred from the saltators to the impact surface. According to Eq. (7), the dust flow is calculated by multiplying the average kinetic energy of the saltators (E_s) by the number of saltators that impact the surface unit in the time unit (n_s), by a given efficiency coefficient (ε) which expresses the mass of dust emitted per unit of kinetic energy transmitted to the impact surface (Eq. 7):

$$F_d = n_s E_s \varepsilon. \quad (7)$$

Many authors (Shao et al. 1993; Duràn et al. 2011; Kok 2010) developed the conceptual relationship expressed by Eq. (7) and suggested the use of Eq. (8) to calculate the dust flow:

$$F_d = C_F \rho_a u_{*it} (u_*^2 - u_{*it}^2). \quad (8)$$

where C_F is a constant measured in kg/j , u_{*it} is the *impact threshold velocity*, u_* is the *friction velocity*, and ρ_a is the fluid density.

As an alternative to the energetic approach, the emitted dust flow can be estimated as a function of the saltation flow Q , according to Eq. (9):

$$F_d = \alpha Q. \quad (9)$$

On that basis, Marticorena and Bergametti (1995) developed the Eq. (10):

$$F_d = C_K \frac{\rho_a}{g} u_*^3 \left(1 - \frac{u_{*it}^2}{u_*^2}\right) \left(1 + \frac{u_{*it}}{u_*}\right). \quad (10)$$

where the constant C_K has dimensions of m^{-1} .

Shao et al. (1996) developed the *Wind Erosion Assessment Model* (WEAM), according to which the one-dimensional flow of particles with d_d diameter is determined by the saltation of particles with d_s diameter, according to Eq. (11):

$$\hat{F}(d_d, d_s) = \left(\frac{\gamma c_b \rho_m d}{\psi}\right) u_*^3 \left[1 - \left\{\frac{u_{*t}(d_s)}{u_*}\right\}^2\right]. \quad (11)$$

where m_d is the mass of the emitted particles, ψ is the binding energy between the particles and the surface, c_b expresses the efficiency of the saltation bombardment, γ is the dimensionless ratio $(U_0 + U_1)/2 \cdot u_*$, U_0 and U_1 are, respectively, the lifting and the impact velocity of the bouncing particles, and u_* and u_{*t} are, respectively, the friction velocity and threshold friction velocity.

The relationships that express the dependence of the vertical flow from the interparticle forces, the size of individual particles, the presence of crusts, the soil moisture content, and its plastic characteristics are not known in explicit and general terms. The influence of those parameters is instead introduced into the formulas in the form of constant values (*site-specific constants*), which are experimentally determined for each specific case study.

That strategy was followed by the authors of a report regarding the air dispersion modelling of the fugitive dust emitted by the red mud basin managed by Alcoa World Alumina in Australia (Air Assessment for Alcoa World Alumina Australia 2005). The authors of the study have elaborated the PM_{10} flow expression suggested by Shao et al. (1996) by replacing in Eq. (12) the friction velocity u_* and the threshold friction velocity u_{*t} , respectively, with the mean wind velocity u and the threshold velocity u_t at 10 m. The parameters that describe the role of the forces acting on the particles (gravity and interparticle forces), the saltators' kinetic energy and the energy transfer efficiency of the bouncing motion (γ , c_b , m_b , ψ) have been incorporated into a single site-specific factor (k). The resulting mathematical model is given by Eq. (12):

$$PM_{10} = k \left[u^3 \cdot \left(1 - \frac{u_t^2}{u^2} \right) \right], \quad \text{per } u > u_t \quad (12)$$

$$PM_{10} = 0, \quad \text{per } u \leq u_t.$$

4 Red Mud Deposits

Red muds are composed of very small and relatively uniform particles (90% under 20 μm) with specific weight in the range between 3.2 and 3.8 g/cm^3 . They are characterized by low values of plasticity index and plastic limit (liquid) and are classified as silts. Until the '70s, red muds were disposed in lagoons, with a solid content around 20–25% (wet disposal); currently, mainly to reduce the environmental impact, they are previously dried to a solid content around 55–75% and then disposed in landfills: dry staking deposits, with water content around 55–65%, and dry disposal deposits, with water content around 65–75%. When disposed in lagoons the red mud is a water suspension; in dry staking is a supersaturated solid (water content higher than the liquid limit); in dry disposal is a plastic solid (water content lower than the liquid limit and higher than the plastic limit).

In none of those disposal conditions wind erosion occurs, as it is inhibited by the particle forces that characterize the supersaturated and plastic states. Under dry

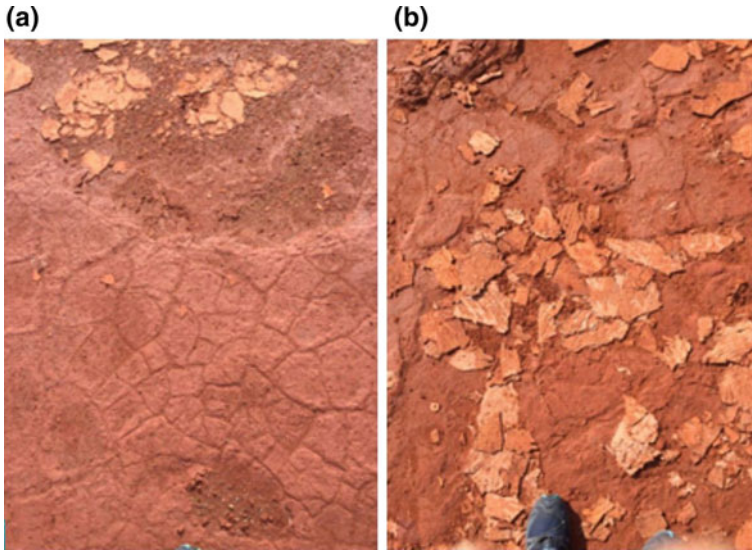


Fig. 3 BRDA surface: **a** mud cracks and particles deposits; **b** particle deposits and crusts

climatic conditions, however, it is possible the undertaking of a drying process that changes the mud into a dried solid: compact rigid crusts a few mm thick are formed at the surface separated by cracks (Fig. 3a), the more widespread and open the higher the initial water content in the mud.

The surface of the crusts does not generate saltators because of the high forces binding the particles inside the dry solid; they are produced instead by:

- the passage of people or vehicles on the surface when the mud is in the plastic state;
- the crushing of dried crusts due to the passage of people or vehicles or mechanical actions (rain, hail, etc.);
- the action of the wind on the crusts' edges (chipping).

Individual particles (type A) and particle aggregates (type B) form a granular material that settles in the mud cracks and in the surface depressions (Fig. 3a, b).

5 Conceptual Emission Model

According to the above description, the following conceptual model can describe the emission of dust from a red mud deposit:

- an initial ON/OFF condition based on the surface water content;
- a subdivision of the basin surface into categories of emitting areas;
- an emission mechanism for each category of emitting areas.

5.1 *ON/OFF Emission Condition and Surface Discretization*

On the basis of the mud water content at the basin surface, it is possible to distinguish:

1. Emission condition (ON), when the mud at the surface is mainly a dry solid ($W < W_p$), so that the surface is formed by the following categories:
 - residual areas in which the mud water content is higher than W_p (Awet);
 - assemblages of A and B particles inside mud cracks and surface depressions (A & B);
 - crust areas (Acrust);
 - crust edges (Achipping);
2. Non-emission condition (OFF), when the mud at the surface is in a plastic state of consistency ($W > W_p$)

5.2 *Emission Mechanism for Each Category of Emitting Areas*

Assemblages A and B particles: the emission from the surface of these deposits follows the model described in Sect. 3.2. The saltation threshold velocity $U_{TA\&B}$ and the vertical flow of dust ($Fd_{A\&B}$) are defined by Eqs. (3) and (12), respectively.

Surface of the crusts: Due to the high particle forces in the dry solid state of the crust, its surface does not produce saltators (except for very high wind speeds). The expulsion of particles from the crust occurs only as a result of the impact of large saltators (over 500 μm) coming from other emitting surfaces and is therefore triggered at a threshold velocity corresponding to that of large saltators (U_{T500}). The vertical flow Fd_{crust} is calculated again with Eq. (12), where k is specific for this type of emission.

Edges of mud crack: The edges of the mud cracks, due to their shape and the fragility of the dry mud, emit particles when they break (chipping). This phenomenon occurs at a threshold wind velocity U_T chipping greater than $U_{TA\&B}$. The particle flow is described again by Eq. (12), with an appropriate value of k . As the wind speed increases and exceeds the threshold speed defined for the three categories of areas, the three flows are superimposed.

Once the A and B particles are exhausted, the surface emits only the particles originated from the chipping of the crust edges. If this flow is neglected, the surface can be assimilated to a finite or exhaustible source of particles. In the case of surfaces in which transport and disposal operations take place, the production of new particles is continuous and the surface constitutes an infinite source of dust.

5.3 Preliminary Verification of the Conceptual Model

The described conceptual model has been partially verified for a 1000×500 m area within a BRDA. The study was aimed at determining the distribution of the categories of emission areas, the threshold velocities ($U_{TA\&B}$, $U_{Tchipping}$, and U_{Tcrust}), the surface roughness z_0 , and the k constants in the relationships that express the vertical flow.

To this end, the following measures were carried out: incidence of the categories of emission areas, wind speed at two different altitudes, particle size distribution of the particle deposits in the BRDA surface, and concentration of PM_{10} upstream and downstream of the emitting surface. Presently, the incidence of the categories of emission areas, the surface roughness z_0 , and the value of the $U_{TA\&B}$ threshold speed have been determined.

An area of 200 m in the direction normal to the wind and 500 m in the direction parallel to the wind has been identified on the BRDA surface. The incidence of the categories of emission areas was determined by dividing this area into 10 m wide and 500 m long longitudinal strips and each strip in 10 m long segments; for each resulting 10×10 m², the incidence of the three categories of areas was evaluated. The resulting average values were wet area 50%; crust area 40%; area with A and B particle deposit 9.8%; and chipping area 0.2%.

The roughness z_0 was obtained from the contemporary measurements of the wind velocity at two heights (u_1 at $z_1 = 2.0$ m and u_2 at $z_2 = 7.0$ m from the basin surface), in conditions of neutral atmospheric stability. Figure 4 shows the trend of the instantaneous wind speed (1 measure every 5 s) and the mean values over $\frac{1}{2}$ h. A mean value of 0.42 mm was calculated with Eq. (13):

$$z_0 = e^{\left(\frac{u_1 \ln(z_2) - u_2 \ln(z_1)}{u_1 - u_2} \right)}. \quad (13)$$

Fig. 4 Instantaneous wind speed (1 measure every 5 s) and mean values over $\frac{1}{2}$ h

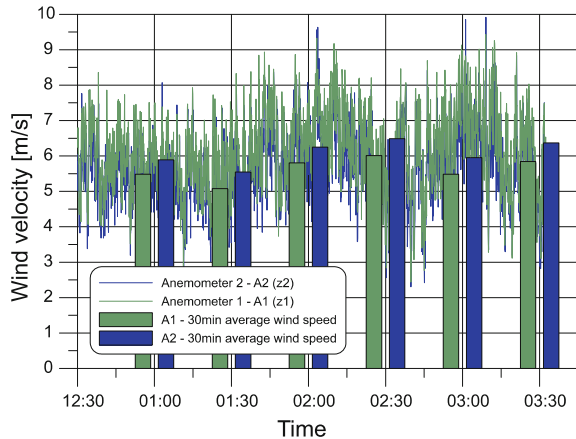


Fig. 5 PM10 concentrations for each wind velocity value (referred at 10 m of height)

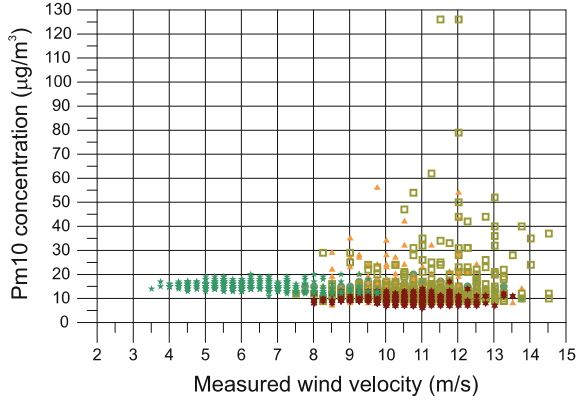
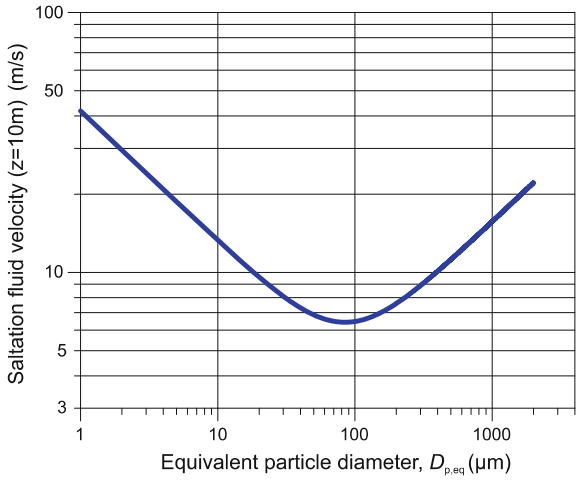


Fig. 6 Saltation velocity at 10 m of height as a function of the saltators' size



The threshold velocity $U_{TA\&B}$ was determined from the PM_{10} concentration measured at the four stations located downwind of the 200×500 m emission area. The obtained $U_{TA\&B}$ was used to have an indication of the saltators' size.

Figure 5 shows the measured PM_{10} concentrations for each wind velocity (measured at 10 m) and indicates that PM_{10} concentration exceeds the background value when the wind speed at 10 m exceeds 8 m/s. This value represents in fact the threshold velocity $U_{TA\&B}$ (the lowest threshold velocity among the three defined emission modes). The size of the saltators that triggers the observed emission is deduced from the Shao formula (3), expressed as shown in Fig. 6, for the threshold velocity of 8 m/s: It results in the range between 30 and 200 μm .

This result is consistent with the particles size distribution of the material in the A&B type areas, where particles under 250 μm are about 27.5% (Table 1).

Table 1 Size distribution of the types A and B particles deposits

Particle size (mm)	+2.0	-2.0 +1.0	-1.0 +0.5	-0.5 +0.25	-0.25
Weight (%)	28.916	13.222	13.864	16.488	27.508

6 Conclusions

This article deals with the emission of PM from the surfaces of the bauxite residue disposal areas (BRDA) exposed to wind erosion. In fact, the examination of the technical and scientific reports has shown that the emission factors proposed for other types of erodible surfaces cannot be directly applied to those deposits, because of their peculiar characteristics: wide and flat surfaces with low roughness and residue physical state dependent on its moisture content.

The action of the wind over the BRDA surfaces has been studied with the aim of developing a conceptual model capable of predicting the conditions that trigger the emission of dust and the emitted flux. The model is based on the observation that the emission occurs only if the mud at the basin surface presents a dry solid physical state and includes three different emission mechanisms related to the presence of loose particle deposits, stiff crusts and mud cracks. The overall potentially emissive surface is first divided into categories of emissive areas; each category is characterized by a set of values, which accounts for the areal extent, the threshold velocity and a k value (parameters included in the flux formula). The overall emission flux can be calculated as the sum of the emission fluxes of each single category of areas for which the threshold velocity and the emission flux have been determined.

The model was applied to a specific case study located in Sardinia. A first experimental phase included the division of the basin surface into categories of emission areas, the calculation of the threshold velocity for the particle deposits ($U_{TA\&B}$) and the calculation of the saltators size. The successive experimental phase is currently under development and includes on site measurements of PM_{10} concentration with higher wind speeds, aimed at evaluating the threshold velocity and the k factors for the other emission mechanisms (crust emission and edge chipping).

Acknowledgements Investigation carried out in the framework of projects conducted by CINIGeo (National Inter-university Consortium for Georesources Engineering, Rome, Italy). “RE-MINE -REstoration and remediation of abandoned MINE sites”, funded by the Fondazione di Sardegna and Regional Sardinian Government (Grant CUP F72F16003160002).

References

Air Assessment for Alcoa World Alumina Australia: Air dispersion modelling of fugitive emissions. Wagerup Refinery (2005)

- Alfaro, S.C., Gaudichet, A., Gomes, L., Maille, M.: Modeling the size distribution of a soil aerosol produced by sandblasting. *J. Geophys. Res.* **102**, 11239–11249 (1997)
- Bagnold, R.A.: The transport of sand by wind. *Geograph. J.* **89**, 409–438 (1937)
- Bagnold, R.A.: *The Physics of Blown Sand and Desert Dunes*. Methuen, New York (1941)
- Chepil, W.S.: Dynamics of wind erosion: II. Initiation of soil movement. *Soil Sci.* **60**, 397–411 (1945)
- Duràn, O., Claudin, P., Andreotti, B.: On aeolian transport: grain-scale interactions, dynamical mechanisms and scaling laws. *Aeolian Res.* **3**, 243–270 (2011)
- Fecan, F., Marticorena, B., Bergametti, G.: Parametrization of the increase of the aeolian erosion threshold wind friction velocity due to soil moisture for arid and semi-arid areas. *Ann. Geophys.* **17**, 149–157 (1999)
- Fletcher, B.: Incipient motion of granular materials. *J. Phys. D Appl. Phys.* **9**, 2471–2478 (1976)
- Iversen, J.D., White, B.R.: Saltation threshold on Earth. *Mars Venus Sedimentol.* **29**, 111–119 (1982)
- Iversen, J.D., Pollack, J.B., Greeley, R., White, B.R.: Saltation threshold on Mars—effect of interparticle force, surface-roughness, and low atmospheric density. *Icarus* **29**, 381–393 (1976)
- Kok, J.F.: An improved parameterization of wind-blown sand flux on Mars that includes the effect of hysteresis. *Geophys. Res. Lett.* **37**, L12202 (2010)
- Kok, J.F., Parteli, E.J.R., Michaels, T.I., Bou, D.: Karam: the physics of windblown sand and dust. *Rep. Prog. Phys.* **75**, 106901 (2012)
- Marticorena, B., Bergametti, G.: Modeling the atmospheric dust cycle: 1 Design of a soil-derived dust emission scheme. *Geophys. Res.* **100**, 16415–16430 (1995)
- Shao, Y.P.: *Physics and Modelling of Wind Erosion*, 2nd edn. Springer, Heidelberg (2008)
- Shao, Y.P., Lu, H.: A simple expression for wind erosion threshold friction velocity. *J. Geophys. Res.* **105**, 22437–22443 (2000)
- Shao, Y., Raupach, M.R., Findlater, P.A.: Effect of saltation bombardment on the entrainment of dust by wind. *J. Geophys. Res.* **98**, 12719–12726 (1993)
- Shao, Y.P., Raupach, M.R., Leys, J.F.: A model for predicting aeolian sand drift and dust entrainment on scales from paddock to region. *Aust. J. Soil Res.* **34**, 309–342 (1996)
- Zingg, A.W.: Wind tunnel studies of the movement of sedimentary material. In: *Proceedings of 5th Hydraulic Conference*, University of Iowa, Iowa City, pp. 111–135 (1953) (*Studies in Engineering Bulletin* 34)